scientific reports

Check for updates

OPEN

Design of retrofit flue gas (CO_2) scrubber for dependable clean energy at the Duvha Coal Power Plant

Hlamalani Innocent Baloyi[1], Leonard U. Okonye[1,2]✉ & Jianwei Ren[2]✉

The coal-fired power sector is facing unprecedented pressure due to the shift to low-carbon energy sources and the need to prevent climate change. It is imperative to incorporate advanced technologies into conventional coal-fired power plants to enhance their efficiency, flexibility, and environmental sustainability. One advantage of post-combustion CCS methods is that they may be retrofitted into power plants that are already in place. The goal of this work is to design a CO_2 flue gas cleaning retrofit system that will meet the most stringent air quality regulations in an operational coal power station in Southern Africa. It will operate and expedite the removal of undesired gas (CO_2) in order to attain ideal requirements for air quality in one of Southern Africa's current coal-fired power plants, the Duvha Coal Power Plant. This study is based on chemical absorption, and explores the mechanistic design of the scrubber, which was accomplished through simple computations and Ansys simulations. The approach for developing a wet CO_2 scrubber and LSTG system is based on chemical absorption and is integrated with a pilot plant. The results of the parametric study provide a foundation for a comprehensive industrial system design for South Africa's coal-powered industry. The results show that the scrubber's cylinder height and diameter can be used for an LSTG system and are appropriate for CO_2 gas flow and capture. The application of the suggested scrubber design and the LTSG's contributions will allow the coal power station to operate with minimal GHG emissions released into the atmosphere. Instead of shutting down coal power facilities, this cleaning system that completely absorbs CO_2 emissions can be used to maintain a robust power infrastructure, rather than being phased out. This will boost the power plant's efficiency over its initial operating efficiency and benefit the nation's economy and the power industry.

Keywords Coal to electricity, Post-combustion, CO_2 capture, Coal-fired power generation, Decarbonize, Flue gas, LSTG, Scrubbing

Coal is the most readily available and economically priced source of energy for power plants in developing nations, including South Africa. Coal power plants, in particular, play a significant role in the generation of end-use applications[1–4]. However, NO_x, SO_2, and CO_2 emissions are included in the flue gas that is created as a byproduct of the combustion process. As greenhouse gases, they have an impact and cause concern about rising environmental pollution, which has an impact on human interactions, food security, habitats of living things, global warming, and agricultural practices. This has led to extensive research on the world's next energy system[2,5–11].

We will continue to rely on thermal electricity for a long time to come, despite the energy system's capacity and share of renewable energy sources having rapidly increased over the past decade to sustain a growing economy. Therefore, constant efforts to lower the quantity of greenhouse gases in the atmosphere are required. By retrofitting the existing units and boosting standards in newly built units based on low-emission and

[1]Department of Mechanical Engineering Science, University of Johannesburg, Cnr Kingsway and University Roads, Auckland Park, Johannesburg 2092, South Africa. [2]Department of Chemical Engineering, University of Pretoria, Cnr Lynnwood Road and Roper Street, Hatfield, Pretoria, 0028, South Africa. ✉email: lokonye@uj.ac.za; jianwei.ren@up.ac.za

high-efficiency recommendations, air pollutant emission concentrations and overall emissions should be lowered even with an increase in coal-fired power[2,4].

The low-carbon energy transition and climate mitigation goals are putting unprecedented pressure on the coal-fired power industry since coal will remain the primary fuel for power generation through 2050. Conventional coal-fired power plants need to be updated with new technologies to become more flexible, efficient, and eco-friendly. Conventional coal-fired power stations already have air pollution control equipment like baghouse filters and electrostatic precipitators installed. These devices collect 90–95% of the dust or fly ash and draw the flue gas component of the waste products from the boiler into the exhaust stacks. However, they do not support the capture of gases like CO_2, SO_2, and NO_x. They are sufficiently effective for gathering fly ash or dust derived from post-combustion waste products; flue gas that exits the stacks is discharged into the atmosphere[8,12]. Installing and developing gaseous cleaning or capture systems that can support an environmentally friendly power infrastructure is therefore urgently needed.

Amongst several coal power plants that are operating in South Africa, the Duvha power plant is a coal-power plant situated in Mpumalanga, which consists of six units (600 MW capacity) with a total size of 3,600 MW. Pulverized coal at the power station is required at 250–300 tons per hour for each unit, amounting to 11.7 million tons (Mt) of coal annually. To improve the efficiency and dependability of the current coal power plants, this work intends to build an advanced and user-friendly wet scrubber LSTG system for CO_2 gas capture for the Duvha power station. With the help of the flue gas scrubbing retrofit system, high emissions from the exhaust stacks will be reduced or eliminated by absorbing CO_2 and clearing away gaseous particles.

Thus, the main goal of this research is to design a flue gas scrubbing system for CO_2 gas capture, that will reduce or completely remove the high emissions emerging from the exhaust stacks[13]. During the switch to renewable energy sources, this tactic enables the coal power plant to run emission-free, without endangering the reliability and efficiency of the current coal-fired power plants. The design will contribute to the existing state of South Africa's power networks, as the CO_2 can be recycled to increase the power/energy plant efficiency. Additionally, the economy may grow since the gas molecule might be utilised to enhance other industrial technologies. South Africa will be able to achieve unprecedented levels of dependability, functionality, efficiency, affordability, and quality of zero-emission electricity, making the research extremely important. This scrubber concept has never been developed and used in the energy sector in Southern Africa. In addition, the data was acquired by professional experience in the energy sector and academic research studies. Since it will provide clearer, more dependable, and more efficient technological means of capturing pollutants (especially gases) that harm the environment and human lives, the design of the CO_2 scrubber will also significantly advance research.

Carbon dioxide (CO_2) capture and separation

Globally, it has been suggested that carbon capture and storage (CCS), a combination of various technologies, is a way of reducing and capturing CO_2 emissions[14–17]. There are three primary methods for reducing carbon dioxide (CO_2) emissions from fossil fuel power facilities, either through pre-combustion, post-combustion, or oxy-fuel combustion approaches[18]. While the pre-combustion process is fully developed, efficient n low adaptation cost, it is however very expensive with traces of impurities (such as H_2S and CO) and often has heat transfer problems. On the other hand, although the oxyfuel combustion process is a relatively simple technology that is suitable for retrofit, the high energy requirement and associated costs hinder its widespread adoption. Although the post-combustion process is a developed technology that can be easily retrofitted to new and existing plants, its high energy demand and low process efficiency coupled with high CO_2 uptake capacity adsorbent requirement to minimise the presence of impurities are drawbacks[14,18]. As a result, a lot of research has been done on the development of innovative CO_2 capture systems. Owing to these serious problems that remain, a great deal of research has gone into developing novel CO_2 capture devices, and various design and optimisation strategies have been used to increase efficiency and promote energy sustainability[6,11,19–33].

The numerous technologies for carbon dioxide separation and capture include absorption, adsorption, membrane, cryogenic distillation, and chemical looping[34,35]. However, adsorption technologies have become more and more popular due to their potential to produce clean energy and improve the environment. The most widespread adsorption method, albeit it has drawbacks, is chemical absorption, which uses solvents based on amines[14,36].

Despite the abundance of CO_2 capture technologies, researchers are still working to develop new approaches that can reduce the energy needed for integration into thermal power plants, as well as the costs associated with CAPEX and OPEX. Post-combustion CO_2 collection is generally regarded as the most flexible and effective technology for integrating with coal-fired power stations without necessitating considerable upgrading[37–39]. Over the past few decades, various technological advancements have considerably increased the efficiency of coal-fired power plants (CFPPs). In light of the energy revolution, China started retrofitting CFPPs to improve power generation efficiency (PGE) by updating generation technologies while lowering air pollution. It has been established that these retrofitting techniques have significantly decreased the emissions of greenhouse gases and air pollutants. These retrofits also increase the plant's self-consumption, maximise heat re-integration into the water steam cycle and lower the scrubbing plant's electrical self-consumption[25,40,41].

Flue gas scrubbing

Since the beginning of the oil industry in the early 1900s, flue gases produced by the combustion of fossil fuels have been cleaned using the scrubbing method. One of the unique techniques for efficiently eliminating CO_2 is amine scrubbing, to ultimately achieve the best or required environmental standards for air quality[31,42–45]. A scrubber and absorber combination can function with a 90% removal efficiency[19,46]. For the amine scrubbing to

be more successful, the CO_2-loaded solvent must be easily regenerated[23,44,47]. The fundamental reaction chemistry between mono-ethanolamine (MEA) and CO_2 is illustrated by the reversible reaction below:

$$2(RNH_2) + CO_2HOT \leftrightarrow RNHCOORNH_3COLD$$

In air pollution control systems, industrial scrubbers are frequently separated into two categories: dry and wet scrubbers. Wet scrubbers employ liquid solvents to remove impurities, whereas dry scrubbers use solid materials to collect gas contaminants emitted by industrial exhaust streams[8,48–50]. Pollutant removal is frequently higher with wet scrubbers than with dry scrubbers. A dry scrubber's gas control effectiveness is less than that of a wet scrubber since it does not saturate the flue gas exhaust (due to moisture treatment). For the removal of dangerous gases, a wet scrubber is recommended over a dry scrubber. There are many different types of wet scrubber packing media, and their composition and consistency will change depending on things like temperature, level of purification, and usage. Wet scrubbers need less maintenance because they are denser and more compact. They might gather both gases and particulate debris, and they lack a backup system for gathering dust[29]. Because the materials might eventually accumulate gases with significant particle mixes, packing towers are frequently used for chemical cleaning and are effective in eliminating contaminated particles. A packed tower may be a practical option even in situations where the contaminated gas stream has a moderate particle density[12,19,29,45,50,51]. Packed bed scrubbers are designed to collect sub-micron particulate matter, smells, and water- or chemically-soluble vapours and fumes generated by industrial processes. Every wet scrubber operates according to the absorption technology concept, which entails exposing the pollutants to the cleaning solution. Packed bed scrubbers employ chemicals to remove contaminants from gas streams so that the cleaning solution can absorb them chemically or physically. In general, packed bed scrubbers cost less than other types of wet scrubbers[30,48,52].

Let-down steam turbine generator boost to the CO_2 scrubber

Unlike a normal CCS retrofit, a "flexible" one has a solvent storage component that allows the generator to remove most of the significant parasitic loads associated with the CO_2 capture process while keeping the CO_2 capture rate constant. After absorbing CO_2 into the solvent at a low temperature, the process releases CO_2 at a high temperature[6,13,21,24,53]. This implies that an operational coal power plant that has a CO_2 scrubber decarburization process installed, requires high-temperature and high-pressure steam which reduces the plant's efficiency. Therefore, it is crucial to reduce the associated energy consumption for CO_2 capture applications[54]. Rather than throttling and cooling down the steam to an ideal pressure and temperature with throttling valves and coolers, eventually recycling exhaust water back to the condenser, the steam from the absorber's reboiler can be propelled by a let-down steam turbine (LSTG) generator. Such improvement is straightforward to implement and control[32,54,55]. From the extracted steam, the LSTG (which generates electricity and lowers carbon intensity when steam pressures are lowered) will recover the excess and increase the efficiency of the current plant. To capture the CO_2 gas and recycle the energy back into the main energy-producing unit, the LSTG will be utilised to increase the excess steam generation[10]. The concept of retrofitting an existing coal power plant with a scrubbing system (with an LSTG improvement), will increase the power generation efficiency by 30%. The factors of release reduction, plant dependability, and cost-effectiveness will ultimately be satisfied, as it is easy to manage and implement[43,54].

CO_2 scrubber design methodology

The separation performance is dependent on a variety of variables, including cycle configuration, temperature and pressure levels, and the number, direction, and order of cycle steps, to build a highly productive cyclic adsorption process[14,56]. Furthermore, one of the crucial components that significantly influences the effectiveness of the cyclic adsorption process is the adsorbent performance. The following are the main design elements that affect the absorption process: the heat duty of the reboiler and condenser, the type, concentration, and flow rate of the absorbent, the pressure during absorption and desorption, and the stage number for the absorber and stripper. Numerous studies on thermally regenerated adsorption systems consider a TSA cycle, which consists of a low-temperature adsorption stage and a high-temperature light product (N_2) purge step[57–63].

This study primarily focuses on the scrubbing mechanism's design and computations. The materials, computations, and formulas utilised in the construction of the proposed CO2 scrubber were derived from the specifications of a typical South African coal-fired power station. The scrubber's exact calculations are necessary since the amount of CO_2 that must be released in the outflow dictates the system parameters. The Duvha coal-fired power plant-specific data, based on the parameters in Table 1, were utilised for the calculations because the design is unique to a single South African plant (additional technical industrial data can be found at https://www.eskom.co.za/heritage/duvha-power-station/). It is assumed that small losses are negligible and that the cleaning system is isothermal. The mechanical design model calculates the technical requirements of the intended CO_2 scrubber (such as sizing, dimensions, height transfer units, flow, internal features of the column, etc.) using a comprehensive engineering formula technique based on the Duvha coal plant data, CO_2 scrubber's technical characteristics and mechanical design. Technical drawings were created with Autocad 2015—English (20.0 s, LMS Tech) covering all pertinent technical and fabrication aspects. Using the engineering simulation and design programme "Ansys-Student" software (2022 R version), was used for the simulation tests using the calculated values.

CO_2 scrubber design considerations

CO_2 is chemically absorbed into a liquid solvent inside the absorber column of a standard post-combustion capture system to separate it from flue gas. The liquid solvent known as the CO_2-rich solvent is directed by solvent pumps into the stripper column. Here, the CO_2 is extracted from the rich solvent and the resulting CO_2 lean solvent is then recycled back into the absorber[11].

Type	Cylindrical vertical packed bed type scrubbing system
Boiler capacity	66,000 kg/hr
Furnace fuel	oil and pulverized coal
Gas load/handling capacity	918.4 m^3/hr
Contents	Air + Acidic vapours
Gas density in kg/m^3	as per calculations
Gas temperature in °C	280 °C
Operating pressure	Ambient (at the point of suction)
Scrubbing liquid	MEA Solution
Pump head	Per design
Solids present in the inlet	Negligible
Desired scheme for scrubbing liquid	Recirculation type
Type of column	Packed column (Raschig Packing)
Column diameter	Per design
Height of Packed bed	Per design
ID fan capacity	Per design capacity
Recirculation pump	Per design

Table 1. Design parameters.

This design process extracts CO_2 from coal-fired power plants using two columns, a scrubber, and a sump tank. As the absorber absorbs the CO_2, the sump tank's job is to refill the solvent so that it may be added back to the absorber. The amount of CO_2 that needs to be contained enters the absorber through its bottom column and rises over one of its two feeds; the kind of flue gas determines how much CO_2 is in the feed. About 3% of CO_2 mol is released into the flue gas from a gas turbine; coal-fired power plants release between 10 and 12% of CO_2 mol, and natural gas-fired power plants release between 5 and 6%[47]. Therefore, this scrubber was designed (see drawing in Fig. 1) based on approximately 10% CO_2 gas per mole of flue gas[47]. The materials that go into making

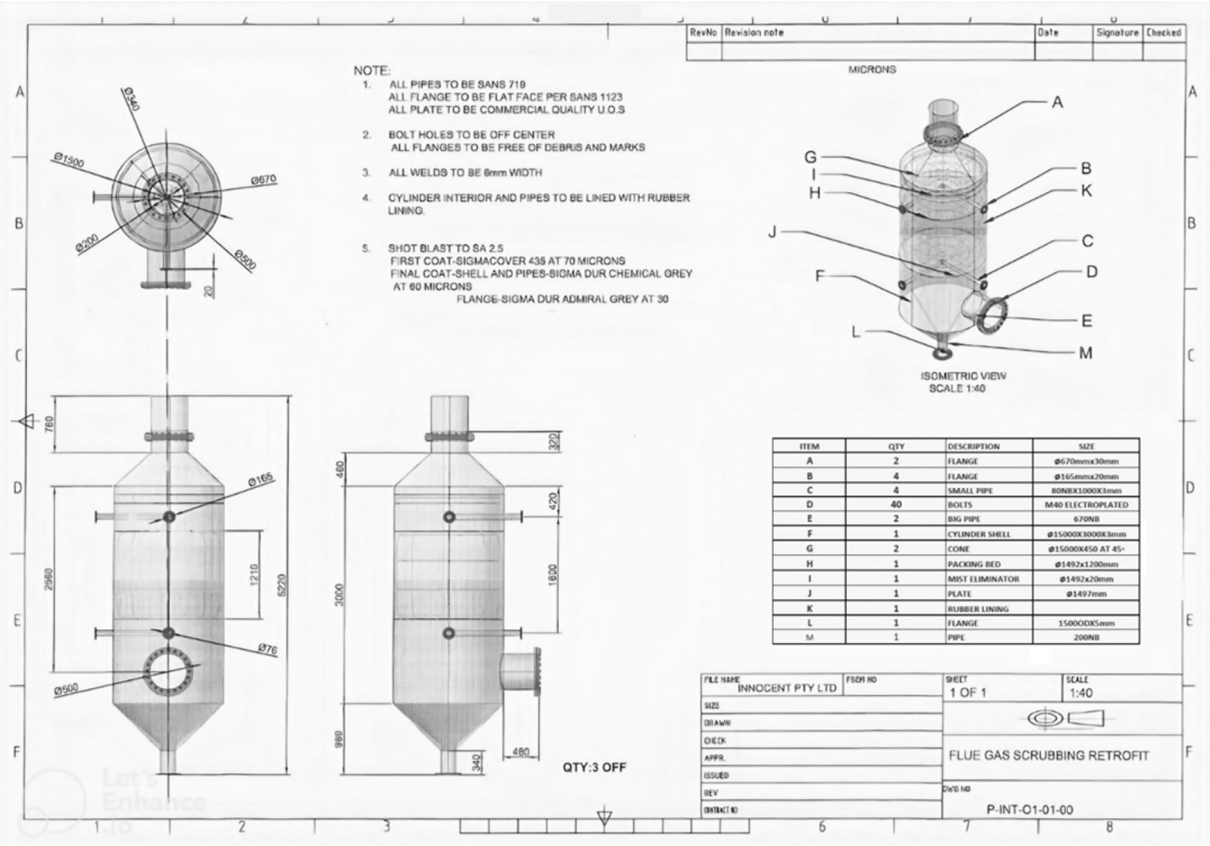

Fig. 1. Isometric view of flue gas scrubbing retrofit.

a scrubber have to be able to withstand harsh environments, like high pressure and temperatures, without losing their mechanical, chemical, or physical qualities[47]. An optimal material packing arrangement is necessary to maximise mass transfer, minimise total scrubber size, and lower pressure drop. Structured packing significantly improved CO_2 removal. Because of dependability and safety issues, the system may be subjected to more stress in the event of anomalous external conditions than was originally anticipated during the design phase. For these reasons, the factor of safety (FOS) for this design was considered to be 1.5. The main process parameters used for this design are highlighted in Table 1 below:

CO_2 scrubber design overview and equations

Equation 1 determines Y_{in} and Y_{out}, the concentrations of pollutants at the input and outflow, respectively, and is used to quantify the separation efficiency and trapping efficacy of the scrubber[64].

$$\eta = \frac{Y_{in} - Y_{out}}{Y_{in}} \tag{1}$$

where η is the overall CO_2 efficiency, Y_{in} is the CO_2 input condition of CO_2 gas, and Y_{out} is the output condition of CO_2 gas.

Based on the volume flow dimensions, the volumetric fraction of the gas, the gas arrangement, and the solvent content, the mass flow of CO_2 gas is computed[65]. The CO_2 gas's mass flow rate, density, and volume were determined using Eqs. 2–4.

For Volume:

$$PV = Mrt \tag{2}$$

where P is the CO_2 gas pressure (2 times the atmospheric pressure was employed because the heat of absorption of CO_2 in MEA is roughly two times that of water vaporisation), V is the volume of 1 mol of CO_2 gas, T is the CO_2 gas temperature, and R is the gas constant (8.314)[26].

For density:

$$\rho = m/V \tag{3}$$

where ρ is the density of CO_2 gas, m is the mass of CO_2 gas, and V is the volume of CO_2 gas.

For the mass flow rate:

$$\dot{m} = \rho Q \tag{4}$$

where, $\dot{m}$ is mass flow rate, ρ is the density of CO_2 gas, and Q is the flow rate of CO_2 gas.

Equations 5 and 6 were used to determine how much urea or MEA solution was needed for decarburization (CO_2 collection) in the CO_2 scrubber design. Based on the movement of material between a boundary plane and an active moving fluid divided by an interface, the mass and heat transfer rate L_{min} were considered. Both forced and natural convection—which happens when temperature variations cause changes in the liquid phase's density—and forced convection were also considered[66]. Equations 5, 6 and 7 explain the concepts of capacity ratio, effectiveness, and the number of transfer units[67–69].

Equation 5 was used to determine the mass and heat transfer rate:

$$Lmin = \frac{z}{1+c}\left[1 - \frac{Y_{out}}{Y_{in}}\right] \tag{5}$$

where: z = gas–liquid ratio, and c = conversion factor determined by the scrubber's stage count.

Water absorbs about 0.3 g CO_2 per kilogramme of water, and the base case solvent had a MEA concentration of 30% on an unloaded basis (Huertas et al., 2015). According to this analysis, the real liquid needed by MEA (L_{min1}) is, therefore, three times L_{min}.

The heating effectiveness (β) Equation yields the necessary MEA liquid and the effectiveness ratio value is typically between 0 and 1[66].

$$(\beta) = \frac{Z\dot{m}}{(1+c)L} \tag{6}$$

where: $\dot{m}$ = mass flow rate, L = MEA liquid required to separate CO_2 gas, z = gas–liquid ratio, c = conversion factor.

The number of heat transfer units

The number of transfer units (NTU) is the measure used to estimate the size of a scrubber. The NTU technique is utilized in mechanical applications if the liquid's exit temperature is unknown, as it is in this instance. Equation 7 displays the formula to determine the NTU value.

$$NTU = \frac{ln\{(1-\eta\beta)/(1-\eta)\}}{1-\beta} \tag{7}$$

where: η is the CO_2 to removal efficiency.

The principle of sizing distillation was applied to determine the flooding ratio in Eq. 10 [48,67,69,70].

$$\left(G_x/G_y\right) = (L_m/\dot{m}) \tag{8}$$

where: G_x = liquid mass flux, G_y = gas mass flux, and L_m = heat transfer rate, $\dot{m}$ = mass flow rate of CO_2 gas.

From the flooding curve, the flooding velocity equation is used to determine the amount of solvent required for the separation process to occur[67,71].

$$\left(G_x/G_y\right)\sqrt{\rho_y/\left(\rho_x-\rho_y\right)} = \text{constant} \tag{9}$$

where ρ_x = density of flue gases, and ρ_y = density of the slurry.

The flooding curve thus summarizes the equation, where the packing factor for the scrubber design was considered[48,69].

$$\frac{G_y{}^2 \times F \times \rho \times \mu_x{}^{0.01}}{G_x(\rho_x - \rho_y)\rho_x} = 0.065 \tag{10}$$

where: Gc = gravitational constant, F = packing factor, μ_x = viscosity of MEA.

The CO_2 Scrubber area and diameter were calculated from Eqs. 11 and 12

$$A = \frac{\dot{m}}{\rho_y V_y} \tag{11}$$

$$A = \frac{\pi D^2}{4} \tag{12}$$

Equation 13 was used to calculate the CO_2 scrubber transfer unit height (HTU), which gauges how well the scrubber packing separates liquids from gases during the liquid-to-gas separation process in the scrubber shell and pipe system. The value of HTU decreases as mass transfer efficiency increases[68,69].

$$HTU = \frac{\dot{m}}{k \times A} \tag{13}$$

where: k is the overall mass transfer coefficient, $\dot{m}$ = mass flow rate and A = Area of pipe. Therefore,

$$\text{Height of tower} = HTU \times \ NTU \tag{14}$$

Pressure drop and frictional losses across CO_2 scrubber pipes

When a fluid encounters frictional forces due to flow resistance as it travels through the tube, a pressure drop happens. Fluid velocity in the pipe and fluid viscosity are the primary causes of fluid flow resistance[66,72–75]. By summing the losses on the pipes and connectors connecting the scrubber to the sump tank, the pressure drop is computed. In contrast, the scrubber design-based friction, pipe length, and pipe diameter are used in Eq. 12 to determine the pipe losses related to solvent circulation. The total losses across the scrubber pipes are determined by adding the fitting and pipe losses. The amount of pressure passing through the scrubber pipe system, or the dynamic head, is then used to compute the pressure drop.

From Eqs. 4 and 11, the velocity is:

$$Vc = \frac{Q}{A} \tag{15}$$

whereas the Reynolds number is obtained using Eq. 16:

$$Re = \frac{Vc \times D}{\nu} \tag{16}$$

where: Vc = velocity of fluid flow, D is the inside diameter of fluid flow, ν = viscosity of the fluid flow.

Laminar and turbulent flows are calculated using the Reynolds number. Laminar flow can be identified by its smooth, continuous fluid motion with a low Reynolds number. High Reynolds numbers generate turbulent flow, which produces chaotic eddies and vortices. Reynolds numbers range from 2300 to 4000 for transitional flow and from 4000 and above for turbulent flow[65]. The pressure loss in a fluid flow is calculated using the dimensionless Darcy friction factor. In calculating the amount of head loss due to friction, the Darcy-Weisbach friction factor (f) must be considered. The Moody Chart[65,72,74–76]. Provided the value of the friction factor. Consequently, the following friction factor equation is applicable for turbulent flow:

$$f = \frac{0.25}{\left\{log\left(\frac{k_1}{3.7\times D} + \frac{5.74}{Re^{0.9}}\right)\right\}^2} \tag{17}$$

where: f = friction factor in the pipe, k_1 = roughness of pipe, D = diameter of the pipe, Re = Reynold's number.

The Pipe frictional losses were obtained using Eq. 18,

$$Kpipe = \frac{f\ell}{D} \tag{18}$$

where K is the pipe frictional losses, ℓ is the length of the pipe (find length on drawing), D is the pipe diameter and f is the friction factor.

Therefore, the total losses in the pipes are calculated using Eq. 19:

$$K_{total} + K_{fittings} + K_{pipe} \tag{19}$$

Fluid passing through pipes creates pipe frictional loss, which is a portion of the total head loss. In fluid flow, head loss is directly correlated with pipe length and tangentially correlated with pipe diameter. The turbulence caused by pipeline components at entrances, exits, and fittings, together with the friction between the fluid and the pipe wall, causes head loss[65]. The pressure drop across pipe Eq. 21 was calculated using the Head loss Eq. 20.

$$HD = \frac{KVc^2}{2g} \tag{20}$$

where: H_D = head loss, g = gravitational acceleration, K = pipe losses, Vc = fluid velocity.

$$P_D = \rho \times g \times H_D \tag{21}$$

CO_2 scrubber design materials' strength (thin wall cylinder)

Thin cylindrical shell structures are an essential structural element that finds numerous practical uses in engineering. The load-bearing capacity of cylindrical shell constructions is mostly dictated by their buckling strength, which is largely reliant on the geometric defects that they display[77–80]. Many industries, such as the mechanical, civil, marine, aerospace, chemical, and power ones, use thin cylindrical shell constructions extensively and with great effectiveness. Thin cylindrical shell shapes are prone to numerous defects as a result of manufacturing problems. These flaws lower these shells' ability to support loads[77,79,80]. An accurate prediction of building buckling is crucial because failure resulting from buckling can be severe. As a result, stability tests are carried out more frequently, and for engineers to produce more accurate calculations, they must be skilled and knowledgeable[77–80].

Stress and strain analysis was conducted on the mild steel material used for the CO_2 scrubber design using Eqs. 22–25.

Circumferential stress θ:

$$\sigma_{\theta=\frac{P\times D}{2t}} \tag{22}$$

Longitudinal stress L:

$$\sigma_{L=\frac{P\times D}{4t}} \tag{23}$$

Circumferential strain ε_θ:

$$\varepsilon_\theta = \frac{(\sigma_{\theta-} \nu\sigma_L)}{E} \tag{24}$$

Longitudinal strain ε_L:

$$\varepsilon_L = \frac{(\sigma_{L-} \nu\sigma_\theta)}{E} \tag{25}$$

CO_2 scrubber design drives

An induced draught (ID) fan and a pump are required to drive the fluid contents. As such calculating the total static head (a sum of static head illustrated in the scrubber drawing and head losses across the pipes) is necessary to determine the power input needed to propel the fluid contents by the induced draught fan. Alongside the performance of the ID fan, fluid density across pipes and flow rate are among the factors that influence the power input.

The static head is given by Eq. 26:

$$H_{total} = H_{s\max} + H_D \tag{26}$$

Having derived the CO_2 flow rate (Q) from the design parameters, therefore, power input of the ID fan is given by Eq. 27:

$$P = \frac{Q \times \Delta H \times g \times \rho_{water}}{Efficiency\%} \tag{27}$$

A power input of 1.5 kW and 230 V for the pipe transfer system is required to pump a flow of MEA solvent into the scrubber, while 250 kW and 400 V are required by the LSTG to recover extra energy back to the main turbines for steam generation.

CO_2 Scrubber design calculations and analysis

CO_2 scrubber calculations

Using Eqs. 1–4, the initial step was to calculate the volumetric concentration of CO_2 gas, density, and mass flow rate. With a minimum separation efficiency (η) of 95%, the amount of CO_2 to be removed (CO_2 output, Y_{out}) from

Eq. 1 is 0.178 mol of CO_2 per kg of air considering that the amount of CO_2 in flue gases is 10%, or 0.1 mol of CO_2 per mole of air (28.8×10^{-3} kg). As a result, CO_2 input (Y_{in}) is 3.57 mol of CO_2 per kg of air. CO_2 gas pressure (P) equals 202.6 kPa given the CO_2 gas temperature (T) of 280 °C (553 K) and the gas constant R = 8.314. Equation 2 gives the density (ρ) of CO_2 gas as 1.27 kg/m^3 and the volume (V) of CO_2 gas as 0.02268 m^3 per mole. The mass flow rate ($\dot{m}$) of CO_2 gas from Eq. 4 is calculated as 19.44 kg/min when the flue gas flow rate of 15.3 m^3/s is used as the CO_2 gas flow rate. These values are summarized in Table 2 below.

Equations 5, 6, and 7 were used to calculate the mass and heat transfer rate, heating effectiveness, and heat transfer unit. The gas-to-liquid ratio (z) from the reaction between MEA and CO_2 is 36 at equilibrium, and the conversion factor (c) is 6, taking into account that material will flow between boundary planes. Equation 5 yields a heat transfer rate (L_{min}) of 94.9 kg/min. However, the actual heat transfer rate (L_{min1}) is 142.5 kg/min based on the minimum value of 1.5, since the actual liquid needed for decarburization is 1.5 to 3 times L_{min}. Equation 6 yields a heating effectiveness/capacity ratio (β) of 0.8. As a result, 7.84 is the number of heat transfer units (NTU) derived from Eq. 7. These values are shown in Table 3 below.

Equations 8–14 were used to calculate the CO_2 scrubber gas velocity, area, diameter, and height of the transfer unit, respectively. Equation 8 yields a flooding ratio (G_x/G_y) of 7.32, however, the flooding curve chat yields 0.3 when Eq. 9 is applied. After determining ρ_x (1.27 kg/m^3), ρ_y (1095 kg/m^3) can be derived using Eq. 9. Equation 10 yields a gas mass flux (G_y) of 1.45 kg/m^{2}s when the gravitational constant (G_c) is 9.81 m^2/s, the packing factor (F_p) is 300 m^{-1} (for 34.3 mm of Raschig[71]), and the viscosity of the MEA solution (μx) is 1.4×10^{-6}. However, because flooding velocity efficacy needs to be between 30 and 50%, the minimum effective gas mass flux (G_y^1) will be 0.435 kg/m^{2}s. Combining Eqs. 4 and 11 yields an effective velocity (V_y^1) of 0.34 m/sec (20 m/min). Following the determination of the scrubber velocity, Eqs. 11 and 12 were used to calculate the scrubber area (A = 0.77 m^2) and diameter (D = 0.995 m). The transfer unit's new diameter (D1) is 1.492 m, and the area (A^1) derived from the new diameter is 1.748 m^2, assuming a safety factor of 1.5. Equation 14 yielded a scrubber height of 3 m since the height of the transfer unit (HTU) from Eq. 13 was found to be 0.37 using a mass transfer coefficient (K) of 30. The calculated parameters taken into account in the design are shown in Table 4.

For the CO_2 scrubber pipes, given a pipe diameter (D^{11}) of 0.076 m and $\dot{m}$ (142.5 kg/min = 2.375 kg/s), from Eqs. 4, 12 and 15, the pipe area (A^{11}), flow rate (Q^{11}) and velocity (V^{11}) were calculated as 0.00454 m^2, 0.002375 m^3/s, and 0.5235 m/s respectively. The pressure drop is calculated by adding the losses on the piping and connections that link the scrubber to the sump tank. Based on the number of entries and bends for the pipes that are a component of the CO_2 scrubber design, the fitting losses total are given (see Table 5). The Reynolds number (Re) of 30,371 was determined by applying the water's viscosity of 1.31×10^{-6} m^2/s to Eq. 16. The Moody diagram[64,72] yielded a value of 0.0025 for the roughness of the pipe (ɛk), and Eq. 19's pipe friction loss (f) is 0.02.

Equation 18 provides the losses in pipes 1 (K_{pipe1}) and 2 (K_{pipe2}), which are 1.742 and 1.435, respectively. According to Eq. 19, the total losses (K_{total}) in pipes 1 and 2 are 5.892 (4.15 + 1.742) and 4.085 (2.65 + 1.435), respectively. Equation 20 yields the following head losses: pipe 1 head loss (H_{D1}) = 0.0823 m; pipe 2 head loss (H_{D2}) = 0.0571 m. As a result, using Eq. 21, the pressure drops (P_D) across the pipes are 807.36 Pa (P_{D1}) and 560.15 Pa (P_{D2}). Table 6 summarises these computed values and indicates that the pressure drop is minimal and enough for optimal system performance.

A mild steel cylindrical scrubber with an internal diameter of 1.492 m, a height of 3 m, a thickness of 4 mm, a Young's modulus (E_y) of 200 GN/m^2, a chamber test pressure of 1 Mpa, and a Poisson's ratio of 0.303 served as the foundation for the CO_2 scrubber design[65].

Parameter	Value
CO_2 input (Y_{in})	3.57 mol
Separation efficiency (η)	95%
CO_2 output (Y_{out})	0.178 mol
Volume of CO_2 (V)	0.02268 m^3
Density of CO_2 (ρ)	1.27 kg/m^3
Mass flow rate of CO_2 ($\dot{m}$)	19.44 kg/min

Table 2. The volumetric concentration of CO_2 gas, density and mass flow rate.

Parameter	Value
Gas to liquid ratio (z)	36
Conversion factor (c)	6
Heat transfer rate (L_{min})	94.9 kg/min
Actual heat transfer rate (L_{min}^1)	142.5 kg/min
Heating effectiveness (β)	0.8
Number of heat transfer units (NTU)	7.84

Table 3. Mass and heat transfer rate, heating effectiveness, and heat transfer unit.

Parameter	Value
Flooding ratio	7.32
Flooding curve	0.3
Slurry density (ρ_y)	1095 kg/m^3
Packing factor (F)	300
MEA viscosity (μ_x)	1.4×10^{-6}
Gas mass flux (G_y)	1.45 kg/m^{2}s
Effective gas mass flux (G_y^1)	0.435 kg/m^{2}s
Effective velocity (V_y^1)	20 m/min
Area (A)	0.77 m^2
Diameter (D)	0.995 m
Safety factor	1.5
New diameter (D^1)	1.492 m
New area (A^1)	1.748 m^2
Height of transfer unit (HTU)	0.37
Scrubber height	3 m

Table 4. CO_2 scrubber gas velocity, area, diameter, and height of transfer unit.

Fitting item	Pipe 1 items	Pipe 2 items	K fittings value	Pipe 1 total	Pipe 2 total
Entrance for pipe	1	1	0.05	0.05	0.05
90 ° Bends	8	5	0.5	4	2.5
Value	1	1	0.1	0.1	0.1
Total				4.15	2.65

Table 5. Fittings losses.

Parameter	Values
Diameter (D^{11})	0.076 m
$\dot{m}$	142.5 kg/min (2.375 kg/s)
Area (A^{11})	0.00454 m^2
Flow rate (Q^{11})	0.002375 m^3/s,
Velocity (V^{11})	0.5235 m/s
Water viscosity	1.31×10^{-6} m^2/s
Reynolds number (Re)	30,371
Pipes roughness (k)	0.0025
Friction loss (f)	0.02
Losses (K_{pipe1})	1.742
Losses (K_{pipe2})	1.435
Total losses (K_{1total})	5.892
Total losses (K_{2total})	4.085
Head loss (H_{D1})	0.0823 m
Head loss (H_{D2})	0.0571 m
Pressure drop (P_{D1})	807.36 *pa*
Pressure drop (P_{D2})	560.15 *pa*

Table 6. Losses and pressure drop across CO_2 scrubber pipes.

$$\text{Limitations}: \ \text{Ratio} = \frac{t}{r} = \frac{4}{0.0536} 0.00536 < 0.01 \text{ s}$$

Equation 22 yields circumferential stress (σ_θ) of 186.5×106 N/m^2 and longitudinal stress (σ_L) of 93.5×106 N/m^2, whereas Eq. 25 yields both circumferential strain (ε_θ) and longitudinal strain (ε_L) of 7.908×10^{-4}.

The total static head (H_{total}) for pipes 1 and 2 is 1.414 m and 1.227 m based on Eq. 26. The static head (H_{smax}) across the reservoir solvent level is 1.32 m (1600 + 720 mm) and 1.16 m (720 + 440 mm) from Fig. 2 drawing.

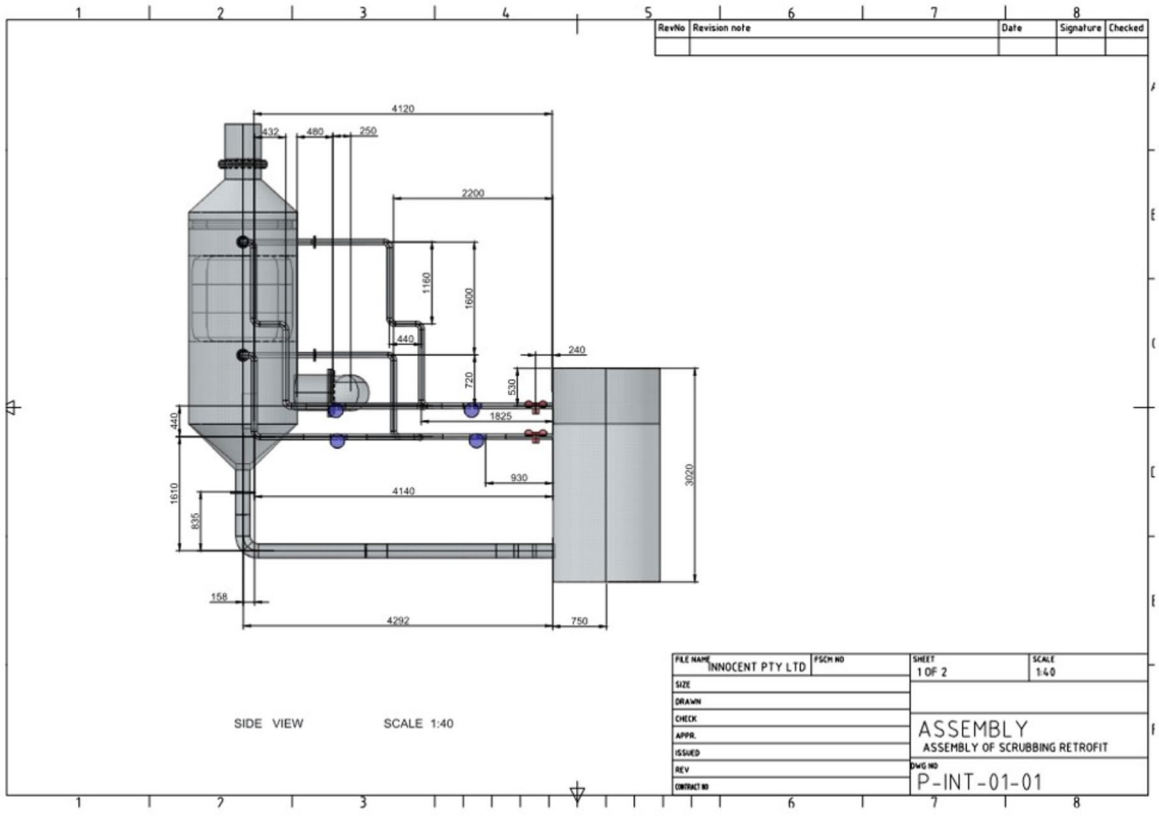

Fig. 2. Scrubber designed for post-combustion CO_2 capture by reactive absorption stripping.

After deriving the CO_2 flow rate (Q) from the design parameters, Eq. 27 calculates the power input of the ID fan needed to convey CO_2 gas by using ρ *water* (1000 kg/m^3), 95% efficiency, Q (0.255 m^3/s) and ΔH = 1.414 m (from static head 1). This results in a power input of 3.723 kW.

According to these calculations for the CO_2 scrubber design, for the decarburization process to take place, 142.5 kg/min of MEA solution and interior dimensions (D) of 1.492 m and height (H) of 3 m are required. Refer to Fig. 1's technical drawing. In conclusion, the results above guarantee that buckling, or instability failure won't happen. Therefore, using the cylindrical shell for the scrubbing system with the specified dimensions is appropriate. The CO_2 scrubber was designed as illustrated in Figs. 1, 2, 3, and 4 (which displays the design schematic) based on these computations and assumptions.

CO_2 scrubber simulation analysis

For this CO_2 scrubber design, 2 D simulation tests (shown in Figs. 5, 6, 7, 8) were carried out using ANSYS using reference values (Table 7) from computations that were utilised to determine the diameter and height of the CO_2 scrubber for the flow and trapping of CO_2. Meshing, which is used to convert unstable shapes into observable volumes, was used to replicate the steady laminar flow in the CO_2 scrubber (Fig. 5a) to enable the results to be displayed precisely in a short amount of time[81].

The two-dimensional (2D) example is adequate to define the flow around a circular cylinder based on each Reynolds number (Re) 300 frames of flow at a time step of dt = 1 s. This is because the velocity field affects the cylinder's surface pressure. Figure 5b depicts a 2D cylinder with arrows pointing in the directions of the wall (green length), cylinder wall, input velocity (blue), and exit pressure (red).

The conditions for convergence for each flow variable—which could be a force, displacement, moment, or rotation—are displayed in Fig. 6. Here, drag force—which is exactly proportional to the inlet velocities—is what drives the iteration's convergence. In fluid dynamics, convergence is the limiting performance that is seen. The real solution to the iterative issue is unknown, but it must nevertheless satisfy the particular accuracy requirement. Figure 6b displays the drag coefficient vs. iteration result calculated from the reference parameters and boundary conditions, whereas Fig. 6a illustrates the inlet velocity vs. iteration results.

To determine the cylinder flow and comprehend the phenomenon of Karman Vortex Street in the steady flow state, the drag force graph (Fig. 6b) was simulated. Karman Vortex Street is an important concept in fluid dynamics because it describes the spinning vortices that result from vortex shedding, which causes the flow separation around the bodies.

The drag flow effect, which is pushed on by a surface dragging over the CO_2 gas, is what causes the effective capturing of the CO_2 gas in a laminar flow when the CO_2 gas inlet pressure is higher than in the cylinder.

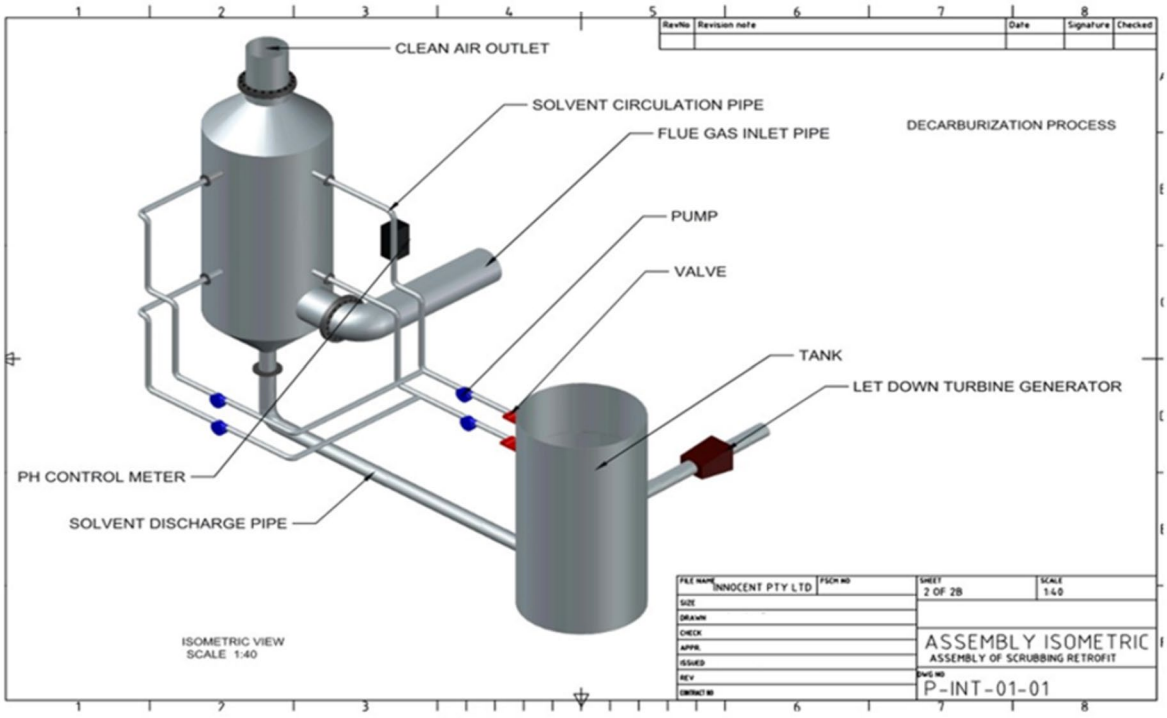

Fig. 3. Isometric view of designed scrubber for post-combustion CO_2 capture.

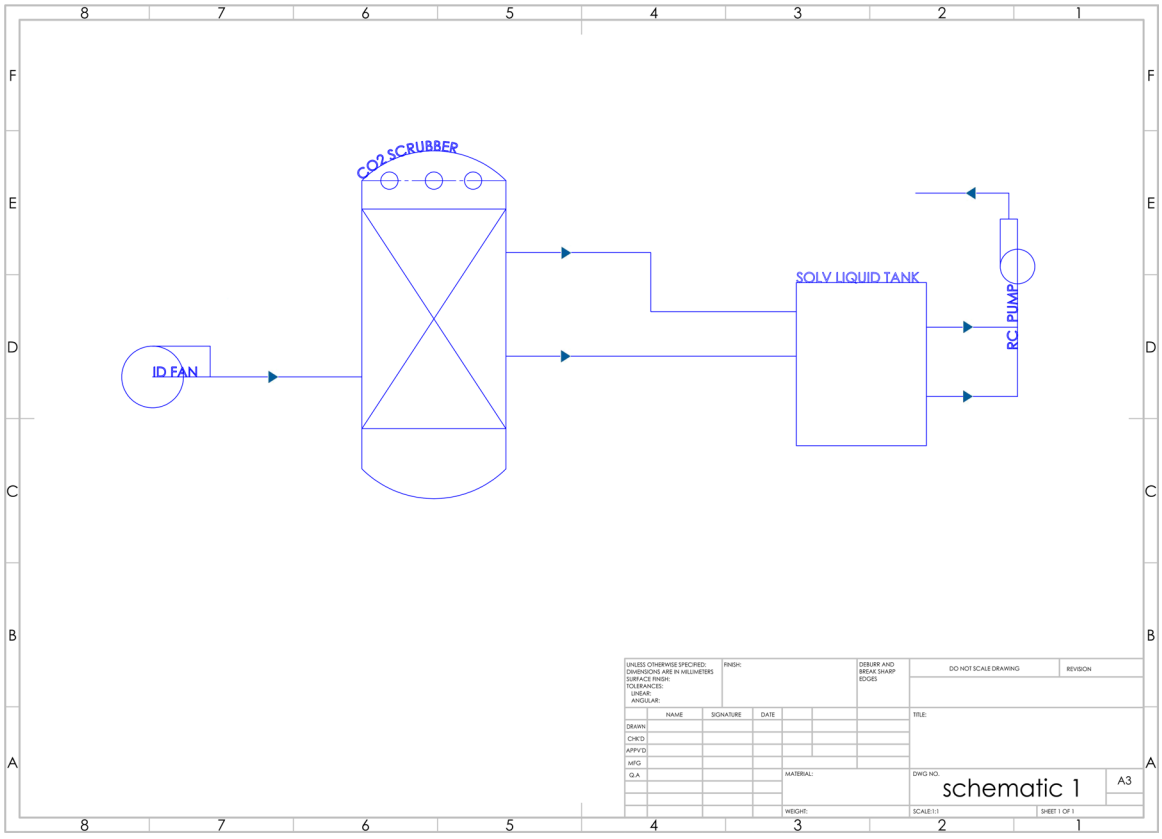

Fig. 4. Scrubber-design schematic for post-combustion CO_2 capture by reactive absorption stripping.

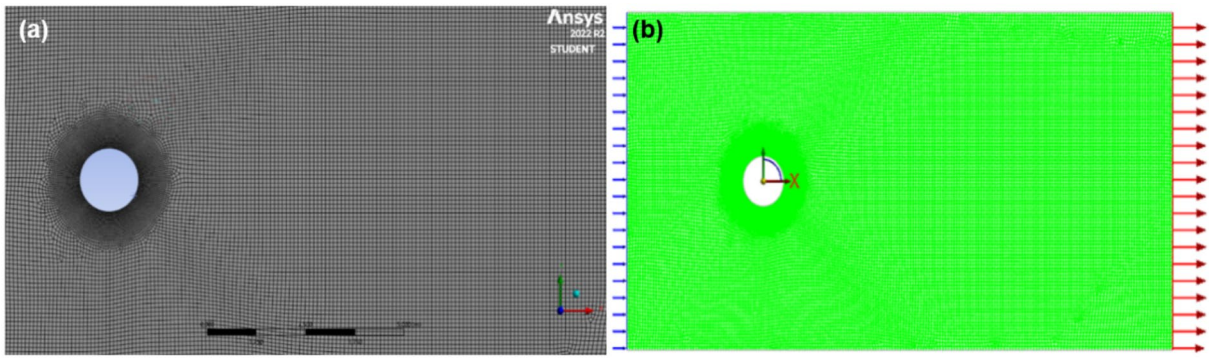

Fig. 5. 2D Scrubber simulation (**a**) Cylinder mesh diagram (**b**) Cylinder flow directions.

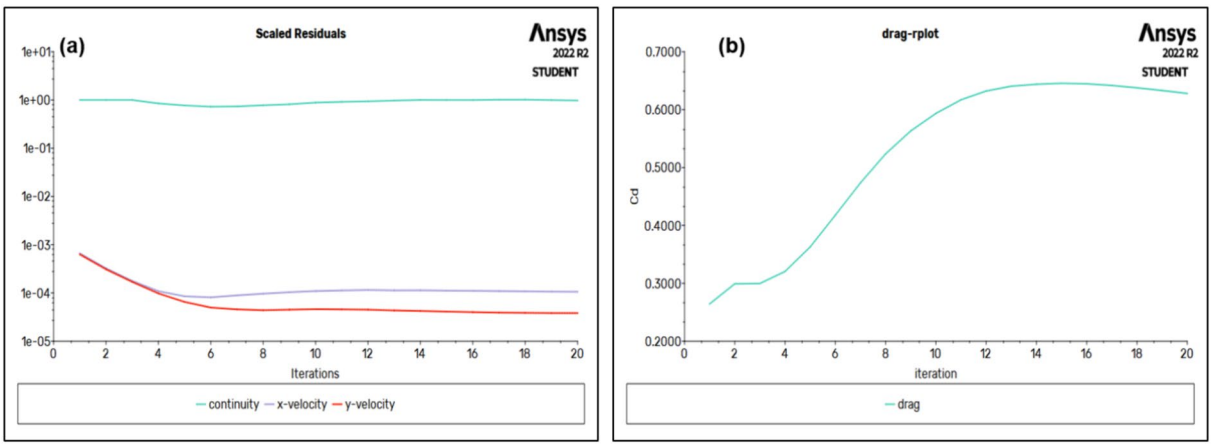

Fig. 6. Simulation graphs (**a**) Velocity vs iteration (**b**) Drag coefficient.

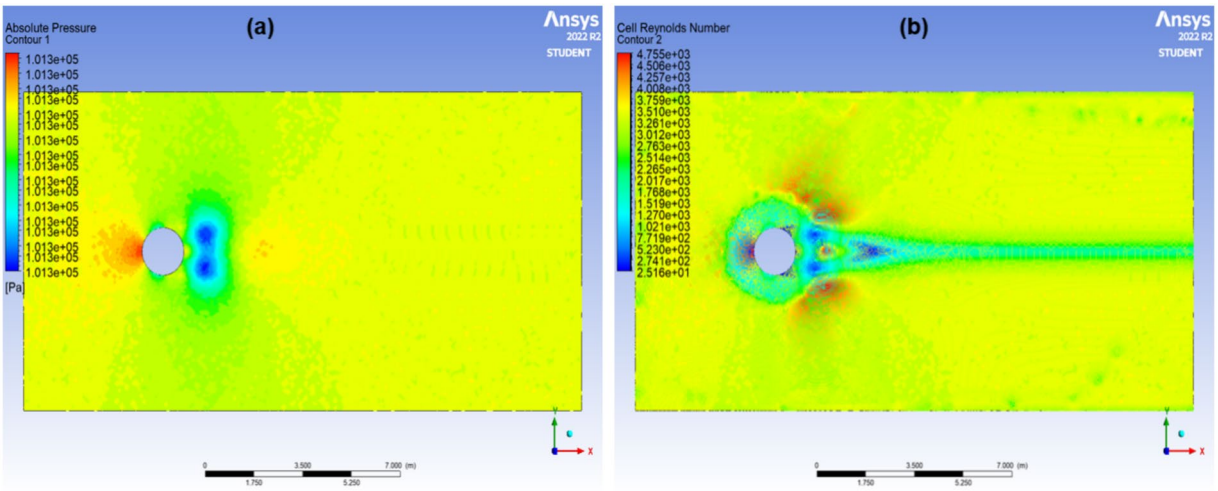

Fig. 7. Pressure simulation (**a**) Absolute Pressure (**b**) Reynold Number.

The Reynolds number is used in flow analysis in cylinders with significant velocity gradients to highlight how important the viscous effect is with the inertia effect, as seen in Fig. 7.

Consequently, Fig. 7a shows the pressure simulation of laminar flow under steady-state conditions inside the scrubber cylinder, whereas Fig. 7b shows how the Reynolds number affects the laminar flow.

The primary variables that affect variations in the pressure coefficient are pressure, geometry, and velocity. The fluid flow's direction and speed as it enters the cylinder from the inlet. Two more illustrations of fluid motion are the streamline and contour velocities in Fig. 8, which demonstrate the flow direction of a tiny volume of fluid.

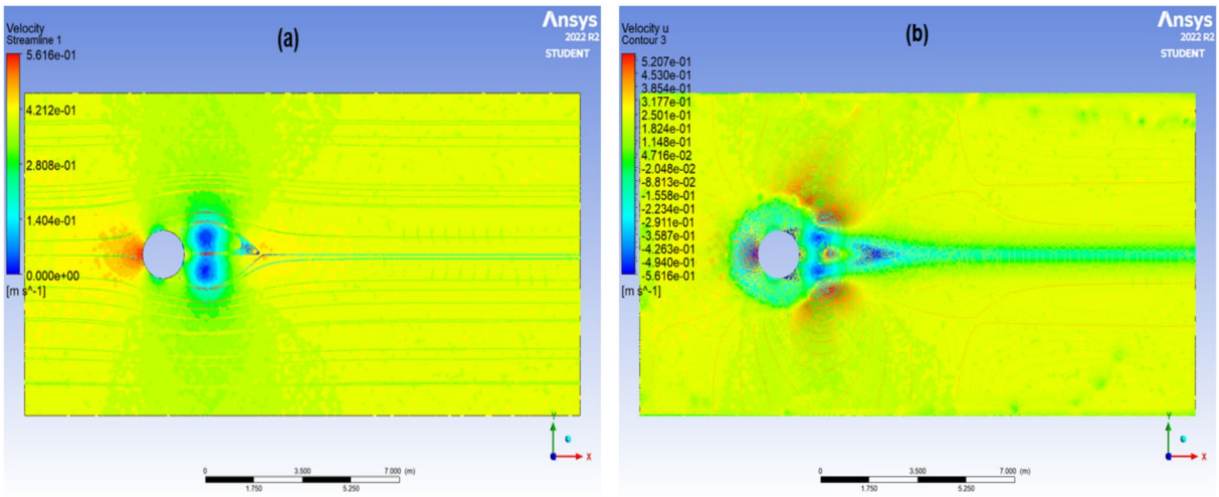

Fig. 8. Velocity simulation (**a**) Streamline (**b**) Contour.

Reference parameter	Boundary values
Fluid	CO_2 gas
Density	1.27 kg/m^3
Temperature	553 K
Scrubber flow diameter	1.5 m
Scrubber height	3 m
Inlet velocity	0.34 m/s
Outlet velocity	The result from the simulation's final step
Inlet pressure	101 300 pascals Ambient pressure
Outlet Pressure	The result from the simulation's final step

Table 7. Reference parameters for simulation analysis.

Since the velocity must always be tangential to the streamline, Fig. 8 models the velocity laminar flow inside the scrubber cylinder under stable conditions.

The simulation of the scrubber design for the 3D statical structural buckling analysis for the scrubber cylinder design was carried out and tested using the reference values in Table 8. Bending deformations may result from a circular movement of the scrubber's cylindrical shell at its limits caused by Poisson expansion and testing pressure. To accurately display the findings' conclusions in a short amount of time, computational solutions, because of their complexity, require mesh precision applied to the full geometry of the scrubber 3D design model (shown in Fig. 9)[78,82].

In the 3D scrubber geometry model, it is assumed that there are only homogenous stresses and that the scrubber cylinder is allowed to extend radially. Make sure there is no local bending in the cylinder before buckling to determine the critical buckling load in the scrubber cylindrical shell. The accompanying 3D model (Fig. 10a) shows the pressure utilised to assess the scrubber's response to buckling. The scrubber body underwent the test seen in the extracted graph in Fig. 10b after being loaded with one MPa of pressure.

The associated 3D model, Fig. 11, illustrates how the scrubber is affected by buckling. The pressure loading did not affect any other area of the cylinder save the cone section. To identify the geometry error that led to

Reference parameter	Boundary values
Modulus elasticity	200 GN/m^2
Poison's ratio	0.303
Scrubber test pressure	1 MPa
Scrubber diameter	1.5 m
Scrubber height	3 m
Scrubber thickness	4 mm

Table 8. Reference parameters for 3D scrubber statical structural buckling analysis.

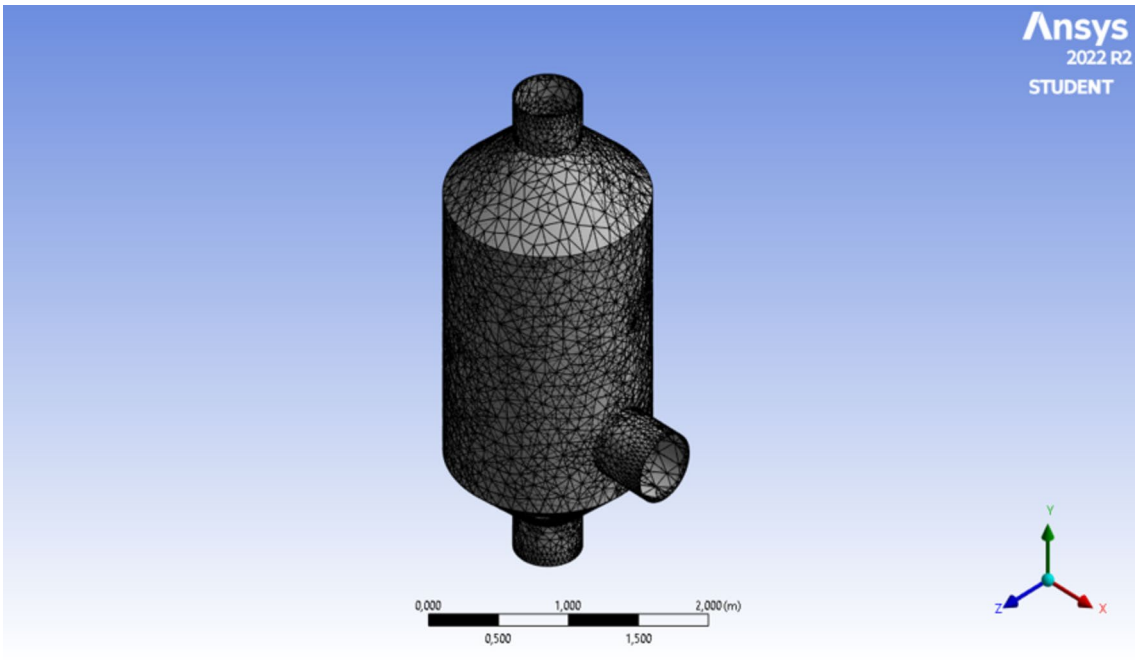

Fig. 9. Mesh 3D scrubber design geometry model for statical structural buckling analysis.

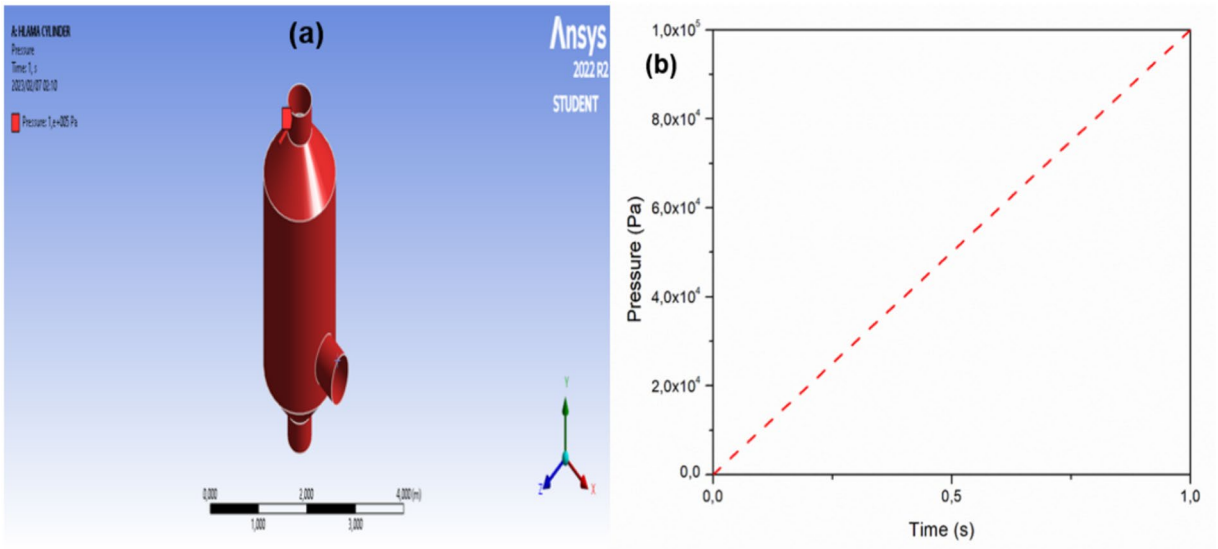

Fig. 10. (**a**) 3D scrubber design geometry for statical structural buckling stress loading (**b**) extracted graph.

the cone's distortion, it is crucial to investigate other situations that might have played a role. Additionally, the findings demonstrate that the scrubber's cylinder diameter and height are suitable for CO_2 gas flow and capture[82].

The results of the 3D simulation analysis diagrams indicate that, as deformation is only visible on the cone-shaped scrubber, buckling only occurred on the scrubber's cone part after a stress of 1 MPa was applied. Buckling did not affect the scrubber cylinder or the pipe's entrance or departure. These findings suggest that the cylinder design is suitable for trapping CO_2 gas.

Conclusion

This study offered a methodology for designing a wet CO_2 scrubber and LSTG system that is integrated with a pilot plant and is based on chemical absorption with aqueous MEA solutions and a column for CO_2 stripping from aqueous MEA solutions. This research attempts to better understand and explore the scrubber's mechanistic design by verifying the gains achieved through basic computations and Ansys simulations. The effects of various flow, pressure, geometry, velocity, and buckling effects were revealed by the simulated parametric analysis that was carried out. A dependable implementation of a two-tank scrubber and LSTG system may be incorporated

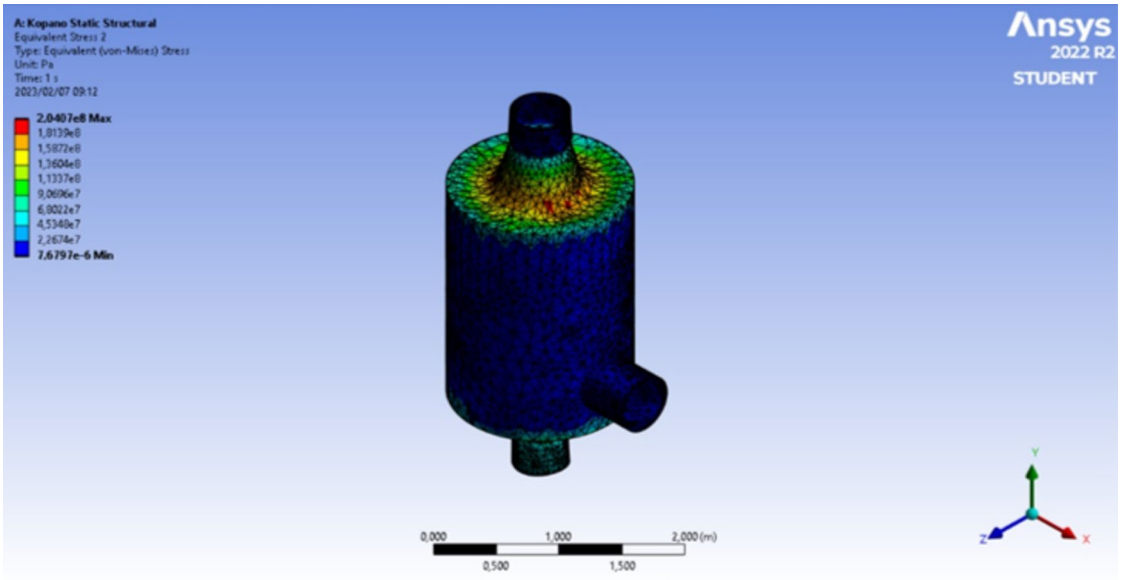

Fig. 11. 3D scrubber design geometry statical structural buckling effect.

into a coal-fired power plant to capture 90–95% of CO_2 purity at the lowest possible cost, according to the results of the parameters that were taken into consideration.

In summary, the study describes how a coal-fired power plant's CO_2 scrubbing system is designed to reduce emissions. Before gradually phasing out coal power plants, the CO_2 scrubbing design places attention on optional constructive options accessible to manage the issues encountered with electricity demand. The present design processes serve as a solid basis for an extensive industrial system design for the coal-powered industry in South Africa. The work evaluated the necessary minimum absorption units, solvent flow rate, column packing, and column size requirements to design a CO_2 scrubber system, based on the industrial data for the Duvha coal power station. The CO_2 gas flow was regarded as stable and laminar based on the outcomes of the 2D simulation analysis diagrams. Additionally, the drag coefficient reached a level that is adequate for cylinder flow—roughly 0.65. As a result, the scrubber's design and the CO_2 gas flow and capture are compatible. The results of the 3D simulation analysis diagrams suggest the scrubber's cone section be assessed, and modified, and that other advanced corrosion applications, such as polymer lining or tiling, be taken into account.

The results of this investigation offer enhanced comprehension of the impact of various factors and their interplay on the reactive absorption stripping scrubber's design performance. More importantly, the approach taken in this work can be used to develop an appropriate reactive absorption stripping scrubber to be used in a post-combustion CO_2 capture system, even though a thorough evaluation would be required. This would enable the utilisation of the current coal-fired power plant infrastructure with modest modifications and retrofitting.

Availability of data and materials

The data sets used and/or analysed during the current study are available on request. Contact: Prof J. Ren (jianwei.ren@up.ac.za).

Received: 19 May 2023; Accepted: 3 September 2024
Published online: 08 October 2024

References

1. Wu, S., Bergins, C., Kikkawa, H., Kobayashi, H. & Kawasaki, T. Technology Options for Clean Coal Power Generation with CO_2 Capture. in *XXI World Energy Congress* 22 (XXI World Energy Congress, Montreal, Canada, 2010).
2. Yang, Y., Li, C., Wang, N. & Yang, Z. Progress and prospects of innovative coal-fired power plants within the energy internet. *Glob. Energy Interconnect.* **2**, 160–179 (2019).
3. Ratshomo, K. South African coal sector report. 34.
4. Zhang, H., Zhang, X. & Yuan, J. Coal power in China: A multi-level perspective review. *WIREs Energy Environ.* **9**, e386 (2020).
5. Costa, C. *et al.* Roadmap for achieving net-zero emissions in global food systems by 2050. *Sci. Rep.* **12**, 15064 (2022).
6. Craig, M. T., Jaramillo, P., Zhai, H. & Klima, K. The economic merits of flexible carbon capture and sequestration as a compliance strategy with the clean power plan. *Environ. Sci. Technol.* **51**, 1102–1109 (2017).
7. Schmidhuber, J. & Tubiello, F. N. Global food security under climate change. *Proc. Natl. Acad. Sci.* **104**, 19703–19708 (2007).
8. Schnelle, K. B. & Brown, C. A. *Air pollution control technology handbook* (CRC Press, 2002).
9. Seneviratne, S. I. *et al.* Changes in climate extremes and their impacts on the natural physical environment: An overview of the IPCC SREX report. 115,122,128 (2012).
10. Tregambi, C. *et al.* Modelling of a concentrated solar power – photovoltaics hybrid plant for carbon dioxide capture and utilization via calcium looping and methanation. *Energy Convers. Manag.* **230**, 113792 (2021).
11. van der Wijk, P. C. *et al.* Benefits of coal-fired power generation with flexible CCS in a future northwest European power system with large scale wind power. *Int. J. Greenh. Gas Control* **28**, 216–233 (2014).
12. Soud, H. N. & Mitchell, S. C. *Particulate Control Handbook for Coal-Fired Plants* (IEA Coal Research, London, 1997).

13. Qvist, S., Gładysz, P., Bartela, Ł & Sowiżdżał, A. Retrofit decarbonization of coal power plants—A case study for Poland. *Energies* **14**, 120 (2020).
14. Karimi, M., Shirzad, M., Silva, J. A. C. & Rodrigues, A. E. Biomass/Biochar carbon materials for CO2 capture and sequestration by cyclic adsorption processes: A review and prospects for future directions. *J. CO2 Util.* **57**, 101890 (2022).
15. Raganati, F., Miccio, F. & Ammendola, P. Adsorption of carbon dioxide for post-combustion capture: A review. *Energy Fuels* **35**, 12845–12868 (2021).
16. Siegelman, R. L., Milner, P. J., Kim, E. J., Weston, S. C. & Long, J. R. Challenges and opportunities for adsorption-based CO2 capture from natural gas combined cycle emissions. *Energy Environ. Sci.* **12**, 2161–2173 (2019).
17. Sumida, K. *et al.* Carbon dioxide capture in metal-organic frameworks. *Chem. Rev.* **112**, 724–781 (2012).
18. Karimi, M., Shirzad, M., Silva, J. A. C. & Rodrigues, A. E. Carbon dioxide separation and capture by adsorption: A review. *Environ. Chem. Lett.* **21**, 2041–2084 (2023).
19. Bai, H. & Yeh, A. C. Removal of CO_2 greenhouse gas by ammonia scrubbing. *Ind. Eng. Chem. Res.* **36**, 2490–2493 (1997).
20. Bishnoi, S. & Rochelle, G. T. Absorption of carbon dioxide into aqueous piperazine: Reaction kinetics, mass transfer and solubility. *Chem. Eng. Sci.* **55**, 5531–5543 (2000).
21. Budzianowski, W. M. Mitigating NH_3 Vaporization from an aqueous ammonia process for CO_2 capture. *Int. J. Chem. React. Eng.* **9**, (2011).
22. Chen, L. *et al.* Temperature swing adsorption for CO2 capture: Thermal design and management on adsorption bed with single-tube/three-tube internal heat exchanger. *Appl. Therm. Eng.* **199**, 117538 (2021).
23. Jassim, M. S. & Rochelle, G. T. Innovative absorber/stripper configurations for CO_2 capture by aqueous monoethanolamine. *Ind. Eng. Chem. Res.* **45**, 2465–2472 (2006).
24. Kang, C. A., Brandt, A. R. & Durlofsky, L. J. Optimal operation of an integrated energy system including fossil fuel power generation, CO_2 capture and wind. *Energy* **36**, 6806–6820 (2011).
25. Li, J. *et al.* China's retrofitting measures in coal-fired power plants bring significant mercury-related health benefits. *One Earth* **3**, 777–787 (2020).
26. Madeddu, C., Errico, M. & Baratti, R. *CO2 Capture by Reactive Absorption-Stripping: Modeling, Analysis and Design* (Springer International Publishing, Cham, 2019). https://doi.org/10.1007/978-3-030-04579-1.
27. Mam'un, S., Svendsen, H. F., Hoff, K. A. & Juliussen, O. Selection of new absorbents for carbon dioxide capture. *Energy Convers. Manag.* **48**, 251–258 (2007).
28. Moazzem, S., Rasul, M. G. & Kh, M. M. K. A review on technologies for reducing CO_2 emission from coal fired power plants. in *Thermal Power Plants* (ed. Rasul, M.) (InTech, 2012). https://doi.org/10.5772/31876.
29. Nuckols, M. L., Purer, A. & Deason, G. A. *Design guidelines for carbon dioxide scrubber*. **73** (1985).
30. Wang, S., Wang, J., Song, C. & Wen, J. Optimization investigation on operating parameters of a scrubbing tower using a genetic algorithm. *Chem. Eng. Technol.* **43**, 2109–2117 (2020).
31. Wang, X. & Song, C. Carbon capture from flue gas and the atmosphere: A perspective. *Front Energy Res* **8**, 560849 (2020).
32. Yoro, K. & Sekoai, P. The potential of CO_2 capture and storage technology in South Africa's coal-fired thermal power plants. *Environments* **3**, 24 (2016).
33. Zhao, L. *et al.* Gas purification in a scrubber tower: Effects of the multilayer tray misalignment. *Case Stud. Therm. Eng.* **55**, 104130 (2024).
34. Canevesi, R. L. S., Andreassen, K. A., da Silva, E. A., Borba, C. E. & Grande, C. A. Pressure swing adsorption for biogas upgrading with carbon molecular sieve. *Ind. Eng. Chem. Res.* **57**, 8057–8067 (2018).
35. Madejski, P., Chmiel, K., Subramanian, N. & Kuś, T. Methods and techniques for CO2 capture: Review of potential solutions and applications in modern energy technologies. *Energies* **15**, 887 (2022).
36. Dhaneesh, K. P. & Ranganathan, P. A comprehensive review on the hydrodynamics, mass transfer and chemical absorption of CO2 and modelling aspects of rotating packed bed. *Sep. Purif. Technol.* **295**, 121248 (2022).
37. Alabid, M. & Dinca, C. Membrane CO2 separation system improvement for coal-fired power plant integration. *Energies* **17**, 464 (2024).
38. Bravo, J. *et al.* Optimization of energy requirements for CO2 post-combustion capture process through advanced thermal integration. *Fuel* **283**, 118940 (2021).
39. Wilkes, M. D. & Brown, S. Flexible CO2 capture for open-cycle gas turbines via vacuum-pressure swing adsorption: A model-based assessment. *Energy* **250**, 123805 (2022).
40. Eguchi, S. CO2 reduction potential from efficiency improvements in China's coal-fired thermal power generation: A combined approach of metafrontier DEA and LMDI. *Energies* **15**, 2430 (2022).
41. Stöver, B., Bergins, C. & Klebes, J. Optimized post combustion carbon capturing on coal fired power plants. *Energy Proc.* **4**, 1637–1643 (2011).
42. Chien, T.-W. & Chu, H. Removal of SO_2 and NO from flue gas by wet scrubbing using an aqueous $NaClO_2$ solution. *J. Hazard. Mater.* **80**, 43–57 (2000).
43. Gibbins, J. R. & Crane, R. I. Scope for reductions in the cost of CO_2 capture using flue gas scrubbing with amine solvents. *Proc. Inst. Mech. Eng. Part J. Power Energy* **218**, 231–239 (2004).
44. Rochelle, G. T. Amine scrubbing for CO_2 capture. *Science* **325**, 1652–1654 (2009).
45. Wei, J., Luo, Y., Yu, P., Cai, B. & Tan, H. Removal of NO from flue gas by wet scrubbing with $NaClO_2$/$(NH_2)_2CO$ solutions. *J. Ind. Eng. Chem.* **15**, 16–22 (2009).
46. Allam, R. J. & Spilsbury, C. G. A study of the extraction of CO_2 from the flue gas of a 500 MW pulverised coal fired boiler. *Energy Convers. Manag.* **33**, 373–378 (1992).
47. Liu, S., Bie, Z., Lin, J. & Wang, X. Curtailment of renewable energy in Northwest China and market-based solutions. *Energy Policy* **123**, 494–502 (2018).
48. Ghadyanlou, F., Azari, A. & Vatani, A. A review of modeling rotating packed beds and improving their parameters: Gas-liquid contact. *Sustainability* **13**, 8046 (2021).
49. IEA. *Putting CO_2 to Use*. https://www.iea.org/reports/putting-co2-to-use (2019).
50. Air Pollution Control Calculations. in *Handbook of Environmental Engineering Calculations* (eds. Lee, C. C. & Lin, S.) (McGraw Hill, New York, 2007).
51. O'Shaughnessy, E., Cruce, J. R. & Xu, K. Too much of a good thing? Global trends in the curtailment of solar PV. *Sol. Energy* **208**, 1068–1077 (2020).
52. Pham, T.-D. *et al.* Emission control technology. in *Current Air Quality Issues* (IntechOpen, 2015). https://doi.org/10.5772/59722.
53. Loftus, P. J., Cohen, A. M., Long, J. C. S. & Jenkins, J. D. A critical review of global decarbonization scenarios: What do they tell us about feasibility?. *WIREs Clim. Change* **6**, 93–112 (2015).
54. Barbour, W., Oommen, R., Shareef, G. S. & Vatavuk, W. M. Post-Combustion Controls. in *EPA Air Pollution cost Control Manual* 60 (1995).
55. Harrell, G. & Jendrucko, R. Steam turbine versus pressure reducing valve operation. *Cogener. Compet. Power J.* **18**, 25–36 (2003).
56. Joss, L., Gazzani, M. & Mazzotti, M. Rational design of temperature swing adsorption cycles for post-combustion CO2 capture. *Chem. Eng. Sci.* **158**, 381–394 (2017).

57. Clausse, M., Merel, J. & Meunier, F. Numerical parametric study on CO2 capture by indirect thermal swing adsorption. *Int. J. Greenh. Gas Control* **5**, 1206–1213 (2011).
58. García, S., Gil, M. V., Pis, J. J., Rubiera, F. & Pevida, C. Cyclic operation of a fixed-bed pressure and temperature swing process for CO2 capture: Experimental and statistical analysis. *Int. J. Greenh. Gas Control* **12**, 35–43 (2013).
59. Hara, N., Taniguchi, S., Yamaki, T., Nguyen, T. T. H. & Kataoka, S. Bi-objective optimization of post-combustion CO2 capture using methyldiethanolamine. *Int. J. Greenh. Gas Control* **122**, 103815 (2023).
60. Konduru, N., Lindner, P. & Assaf-Anid, N. M. Curbing the greenhouse effect by carbon dioxide adsorption with Zeolite 13X. *AIChE J.* **53**, 3137–3143 (2007).
61. Liu, Z. *et al.* Zeolite Apgiia for adsorption based carbon dioxide capture. *Sep. Sci. Technol.* (2013).
62. Mason, J. A., Sumida, K., Herm, Z. R., Krishna, R. & Long, J. R. Evaluating metal–organic frameworks for post-combustion carbon dioxide capture via temperature swing adsorption. *Energy Environ. Sci.* **4**, 3030–3040 (2011).
63. Rezaei, F. *et al.* Modeling of rapid temperature swing adsorption using hollow fiber sorbents. *Chem. Eng. Sci.* **113**, 62–76 (2014).
64. Huertas, J. I., Gomez, M. D., Giraldo, N. & Garzón, J. CO_2 absorbing capacity of MEA. *J. Chem.* **2015**, 1–7 (2015).
65. Cengel, Y. *Thermodynamics: An Engineering Approach* (Mcgraw-Hill, 2012).
66. *Perry's Chemical Engineers' Handbook*. (McGraw-Hill, New York, 2008).
67. Nitsche, M. & Gbadamosi, R. *Practical Column Design Guide* (Springer International Publishing, Cham, 2017). https://doi.org/10.1007/978-3-319-51688-2.
68. Sinnott, R. K., Coulson, J. M. & Richardson, J. F. *Chemical Engineering Design*. (Elsevier Butterworth-Heinemann, 2005).
69. Theodore, L. & Ricci, F. *Mass Transfer Operations for the Practicing Engineer*. (Wiley, Hoboken, 2010). https://doi.org/10.1002/9780470602591.fmatter.
70. Towler, G. & Sinnott, R. Chapter 17–Separation Columns (Distillation, Absorption, and Extraction). in *Chemical Engineering Design*, 2nd edn (eds. Towler, G. & Sinnott, R.) 807–935 (Butterworth-Heinemann, Boston, 2013). https://doi.org/10.1016/B978-0-08-096659-5.00017-1.
71. Sinnott, R. K. *Chemical Engineering Design* Vol. 6 (Pergamon Press, Oxford, 1993).
72. Brandt, M. J., Johnson, K. M., Elphinston, A. J. & Ratnayaka, D. D. Chapter 14 - Hydraulics. in *Twort's Water Supply* 7th edn (eds. Brandt, M. J., Johnson, K. M., Elphinston, A. J. & Ratnayaka, D. D.) 581–619 (Butterworth-Heinemann, Boston, 2017). https://doi.org/10.1016/B978-0-08-100025-0.00014-4.
73. Hicks, T. G. & Chopey, N. P. *Handbook of Chemical Engineering Calculations*, 4th edn. (McGraw Hill, 2012).
74. Menon, E. S. & Menon, P. S. Chapter 4—Pressure Loss through Piping Systems. in *Working Guide to Pumps and Pumping Stations* (eds. Menon, E. S. & Menon, P. S.) 69–111 (Gulf Professional Publishing, Boston, 2010). https://doi.org/10.1016/B978-1-85617-828-0.00004-4.
75. Ricketts, J. T., Loftin, M. K. & Merritt, F. S. *Standard Handbook for Civil Engineers*. (McGraw-Hill Education, 2004).
76. Moody, L. F. & Moody, L. F. Friction factors for pipe flow. *Trans. Am. Soc. Mech. Eng.* **66**, 671–681 (1944).
77. Elso, M. I. Finite Element Method studies on the stability behavior of cylindrical shells under axial and radial uniform and non-uniform loads made in. (Hochschule Niederrhein University of Applied Sience, 2012).
78. Hu, Z. & Hassan, M. M. Effect of Poisson's ratio on material property characterization by nanoindentation with a cylindrical flat-tip indenter. *J. Mater. Res.* **34**, 10–15 (2019).
79. Prabu, B., Raviprakash, A. & Rathinam, N. Parametric study on buckling behaviour of thin stainless steel cylindrical shells for circular dent dimensional variations under uniform axial compression. *Int. J. Eng. Sci. Technol.* **2**, 134–149 (2010).
80. Vasilikis, D. & Karamanos, S. A. Stability of confined thin-walled steel cylinders under external pressure. *Int. J. Mech. Sci.* **51**, 21–32 (2009).
81. Yunus A. Çengel, Michael A. Boles. *Thermodynamics an Engineering Approach* 7th edn (McGraw-Hill, 2006).
82. Simitses, G. J., Shaw, D., Sheinman, I. & Giri, J. Imperfection sensitivity of fiber-reinforced, composite, thin cylinders. *Compos. Sci. Technol.* **22**, 259–276 (1985).

Acknowledgements

We are grateful for the support from the University of Johannesburg and the National Research Foundation (Grant number: PSTD2204275066).

Author contributions

H.B. came up with the proposal that was presented, and L.U.O. and J.R. discussed and approved it. H.B. did the computations, developed the theory, and wrote the first draft. The paper was written by L.U.O., who also verified the computations and processes. The project was supervised by J.R. and L.U.O. Each author reviewed, edited, and approved the final manuscript.

Funding

This research was not funded.

Competing interests

The authors declare no competing interests.

Additional information

Correspondence and requests for materials should be addressed to L.U.O. or J.R.

Reprints and permissions information is available at www.nature.com/reprints.

Publisher's note Springer Nature remains neutral with regard to jurisdictional claims in published maps and institutional affiliations.